Published in final edited form as:
*Biochemistry*. 2005 June 14; 44(23): 8428–8437. doi:10.1021/bi0480584.

# DNA Damage Induced Hyperphosphorylation of Replication Protein A. 1. Identification of Novel Sites of Phosphorylation in Response to DNA Damage†

**Jonathan E. Nuss**‡, **Steve M. Patrick**‡, **Greg G. Oakley**§, **Gerald M. Alter**‡, **Jacob G. Robison**§, **Kathleen Dixon**§, and **John J. Turchi**[*,‡]
Department of Biochemistry and Molecular Biology, Wright State University, School of Medicine, Dayton, Ohio 45435 and Department of Environmental Health, University of Cincinnati College of Medicine, Cincinnati, Ohio 45267

## Abstract

Replication protein A (RPA) is the predominant eukaryotic single-stranded DNA binding protein composed of 70, 34, and 14 kDa subunits. RPA plays central roles in the processes of DNA replication, repair, and recombination, and the p34 subunit of RPA is phosphorylated in a cell-cycle-dependent fashion and is hyperphosphorylated in response to DNA damage. We have developed an in vitro procedure for the preparation of hyperphosphorylated RPA and characterized a series of novel sites of phosphorylation using a combination of in gel tryptic digestion, SDS–PAGE and HPLC, MALDI-TOF MS analysis, 2D gel electrophoresis, and phosphospecific antibodies. We have mapped five phosphorylation sites on the RPA p34 subunit and five sites of phosphorylation on the RPA p70 subunit. No modification of the 14 kDa subunit was observed. Using the procedures developed with in vitro phosphorylated RPA, we confirmed a series of phosphorylation events on RPA from HeLa cells that was hyperphosphorylated in vivo in response to the DNA damaging agents, aphidicolin and hydroxyurea.

Replication protein A (RPA)[1] is the major eukaryotic single-stranded DNA (ssDNA) binding protein. RPA is a heterotrimeric protein composed of 70, 34, and 14 kDa subunits and was discovered as an essential component of the SV40 cell free DNA replication system (1, 2). RPA's role in DNA replication is to bind and stabilize ssDNA and to stimulate DNA polymerase α (3). Central roles have also been discovered in nucleotide excision repair, DNA mismatch repair, DNA recombination, and the nonhomologous end joining pathway for repair of DNA double strand breaks (4–8). RPA-coated ssDNA also appears to be a key structure for the activation of checkpoint signaling in response to DSBs and stalled DNA

†This work was supported by Public Health Service Grant CA82741 and Grant CDMRP OC020223 to J.J.T. and Public Health Service Grants NS34782 and ES06096 and a research grant from the A-T Children's Project to K.D.



*To whom correspondence should be addressed. Phone: (937)-775-3595; fax: (937)-775-3730; john.turchi@wright.edu.
‡Wright State University.
§University of Cincinnati College of Medicine.

[1]Abbreviations: RPA, replication protein A; XPA, xeroderma pigmentosum group A protein; ssDNA, single-stranded DNA; dsDNA, double-stranded DNA; CIP, calf intestinal phosphatase; PAGE, poly-acrylamide gel electrophoresis; OB, oligonucleotide/oligosaccharide binding; DBD, DNA binding domain; CHCA, α-cyano-4-hydroxy cinnamic acid.

replication (9, 10). In all of these pathways, RPA binds to single-stranded regions of DNA and interacts with a variety of proteins that ultimately govern how genetic information is copied, repaired, and maintained.

Structurally, RPA is composed of multiple homologous domains classified as oligonucleotide/oligosaccharide binding (OB) folds (11). The bulk of RPA's DNA binding activity has been attributed to two OB folds present in the central region of RPA-p70. These two DNA binding domains are termed DBD A and B and the structure of which has been solved by X-ray crystallography in the presence and absence of DNA (11, 12). Evidence also suggests that the central domain of RPA-p34 and the C-terminal domain of RPA-p70, DBDs D and C, respectively, may contribute to DNA binding affinity (13).

It is well documented that RPA is phosphorylated in vivo with the N-terminus of RPA-p34 being the most well characterized region of RPA modification (14, 15). Normally cycling HeLa cells show two RPA-p34 bands separated by single dimensional SDS–PAGE. These phosphorylated species of RPA have been termed Form 1, which migrates at the same molecular weight as calf intestinal phosphatase (CIP)-treated RPA-p34 and Form 2, which migrates as a slightly larger molecular weight species. Peptide mapping studies indicate that phosphorylation occurs primarily at serines 23 and 29, which are consensus sequence sites for cyclin B/$p34^{cdc}$ kinase (15). A higher molecular weight band, Form 3, was recently discovered by arresting HeLa cells at the $G_2$/M transition; this is the major form of RPA as cells progress through mitosis and is referred to as mitotic RPA (16). Additional phosphorylated RPA-p34 forms can be observed following DNA damaging events. These hyperphosphorylated RPA species are characterized by additional RPA-p34 bands observed upon SDS–PAGE analysis with the majority of the subunits present as Form 5 (17). The PI-3 kinases DNA-PK, ATM, and ATR have been implicated in the phosphorylation events responsible for these higher molecular weight species (9, 18–21). Seven potential sites of phosphorylation (serine 4, serine 8, serine 11, serine 12, or serine 13, threonine 21, serine 23, serine 29, and serine 33) exist on the N-terminus of Form 5 RPA-p34 in vitro and in vivo (15). It has yet to be addressed if there are other sites of phosphorylation on the RPA p34 subunit. While phosphorylation of p70 in yeast has been observed (22–25), there have been no reports of phosphorylation of the mammalian RPA p70 subunit. There are also no reports of modification of the p14 subunit of RPA.

In this report, we have identified a series of phosphorylation sites on human RPA p70 and p34 that are observed in an in vitro phosphorylated RPA and also on RPA phosphorylated in vivo in response to DNA damage induced replication fork arrest. These results reveal that phosphorylation is not restricted to the N-terminus of p34 and that additional sites of phosphorylation occur and may contribute to regulation of RPA activity in DNA metabolic pathways.

## MATERIALS AND METHODS

### Materials

Sequencing-grade trypsin and calf intestinal alkaline phosphatase were purchased from Roche (Indianapolis, IN). The energy absorbing matrix, α-cyano-4-hydroxy-cinnamic acid

(CHCA) and trifluoroacetic acid (TFA) were purchased from Sigma (St. Louis, MO). Novex colloidal Coomassie Blue was purchased from Invitrogen (Carlsbad, CA). HPLC-grade acetonitrile was from Fisher Scientific (Fairlawn, NJ). All other reagents were from standard suppliers. Phosphospecific antibodies to serines 4, 8 and serine 33 were purchased from Bethyl Laboratories (Montgomery, TX), and the threonine 21 phosphospecific antibody was provided by Lees-Miller (26). The anti-RPAp34 antibody (RPA/p34 Ab-1) was from Neomarkers (Freemont, CA).

## Cell Lines and Treatments

HeLa cells were obtained from American Type Culture Collection (ATCC; Manassas, VA) and maintained at 37 °C and 5% $CO_2$ in Dulbecco's Modified Eagles medium (DMEM; Gibco, Gaithersburg, MD) supplemented with 10% fetal bovine serum (FBS; Hyclone, Logan, UT) and 1% penicillin–streptomycin (Gibco). Cells were synchronized in S-phase of the cell cycle as previously described (17). To synchronize in S-phase, cells were incubated in growth medium containing aphidicolin (final concentration of 1 $\mu$M; Sigma-Aldrich) for 15 h. Following incubation, the aphidicolin-containing medium was removed; cells were washed with PBS and then incubated in fresh medium without aphidicolin for an additional 2 h at 37 °C. For UV exposure of S-phase synchronized HeLa cells, the growth medium was removed (and held at 37 °C) and cells were washed with phosphate buffered saline (PBS). The PBS was replaced with minimum essential medium (MEM; Gibco) without phenol red, and cells were treated with 20 J/$m^2$ using a low-pressure mercury lamp (Mineralight lamp; model UVG-11; UVP, Inc., San Gabriel, CA) with a maximal output at 254 nm. Following UV exposure, the MEM was removed and replaced with the original growth medium, and cells were allowed to recover for 8 h at 37 °C before harvesting. For hydroxyurea (HU; Sigma-Aldrich, St. Louis, MO) treatment of S-phase synchronized cells, cells were incubated in growth medium containing HU (2 mM) for 3 h before harvesting. The control HeLa cells were synchronized in S-phase but were not treated with UV or HU.

## Protein Purification

Recombinant human RPA (rhRPA) was purified as previously described (27). In vitro hyperphosphorylated RPA was purified by incubating partially purified rhRPA extracted from *Escherichia coli* with HeLa cell extracts supplemented with okadaic acid, microcystin, cantharidin, and *p*-bromotetramisole to inhibit protein phosphatases within the extracts. The kinases within the HeLa cell extracts phosphorylate rhRPA, and the resulting phosphorylated RPA was purified using the same procedure to purify rhRPA. Extracts prepared from HU-treated cells were used to purify in vivo hyperphosphorylated RPA using procedures identical to those described above.

## Electrophoresis and Western Blot Analysis

Single-dimensional SDS–PAGE separations were performed on 13% separating gels and were either stained with Coomassie Blue or transferred to Immobilon P polyvinyl-divinyl fluoride (PVDF) membranes (Millipore, Bedford, MA) at 20 V, 500 mA for 1 h. Membranes were probed with the indicated primary antibody and horseradish peroxidase conjugated secondary antibody. Bound antibodies were visualized using chemiluminescent detection.

### Exhaustive Proteolysis of RPA

For exhaustive digestion of RPA in solution, RPA was incubated in 25% acetonitrile for 30 min at 37 °C, the sample was then diluted to 10% acetonitrile with hydrolysis buffer and trypsin added to a concentration of 1/40 of RPA by weight. The reaction was incubated overnight at 37 °C. Proteolysis of specific RPA subunits was also performed following separation of 10 $\mu$g of protein on a 10% acrylamide/tricine SDS gel. The gel was stained by colloidal Coomassie Blue (Novex), and the individual bands corresponding to the three subunits of RPA were excised with a razor blade. After SDS and stain were removed, the subunits were exhaustively digested with trypsin. All digests were performed in 25 mM ammonium bicarbonate buffer (pH 8).

### HPLC Separation of Tryptic Peptides

HPLC separation of peptides was performed using a 250 × 4.6 mm HI Pore reverse phase C4 column (Bio-Rad). After the tryptic digests were loaded, the column was washed with 5 mL of double-deionized water and the peptides were eluted from the column using a 30 mL linear gradient from 0 to 50% acetonitrile in 0.1% trifluoroacetic acid (TFA). Fractions (0.5 mL) were collected, dried, and suspended in 40 $\mu$L of 25 mM ammonium bicarbonate/10% acetonitrile (pH 7.8) and then analyzed by MALDI-TOF MS.

### MALDI-TOF MS Analysis of HPLC-Purified Peptides

The molecular weight of the tryptic peptides was determined by MALDI-TOF MS. Typically, 1 $\mu$L of each fraction was pipeted onto one spot of an eight spot gold chip (Ciphergen), and samples were allowed to air-dry at room temperature and 0.5 $\mu$L of 2% TFA was added to each dried sample. This spot was then mixed on site with 0.5 $\mu$L of 33 mM α-cyano-4-hydroxy cinnamic acid (CHCA). CHCA was prepared by dissolving the solute in a solvent consisting of 50% acetonitrile, 50% methanol with TFA added to a final concentration of 2%. The samples were then thoroughly air-dried before analysis. Mass spectra were recorded by varying the laser intensity until a satisfactory signal-to-noise was achieved. Using these settings, a minimum of 50 individual spectra were collected to produce an average spectrum.

In spectra in which putative phosphorylation patterns were observed, fractions were spotted in duplicate and CIP was added to one spot to catalyze the dephosphorylation of the peptide. Prior to use, CIP was dialyzed versus 25 mM ammonium bicarbonate pH 7.8 to remove glycerol. CIP reactions were performed by adding 1 $\mu$L (1 unit) of CIP directly to the sample, and the reaction was allowed to proceed for 30 min at room temperature by placing the chip in a humidity chamber. Reactions were terminated by allowing the solution to dry, and the CHCA matrix was then added to each spot as described above.

### Cell Lysate Preparation and Immunoprecipitation

Following HU and UV treatment, HeLa cells were harvested and lysed using a buffer containing 50 mM Tris-HCl, pH 7.5; 150 mM NaCl, 0.1% NP-40; 5 $\mu$g/mL pepstatin, 5 $\mu$g/mL leupeptin; 5 $\mu$g/mL aprotonin, 10 mM NaF, 10 mM $\beta$-glycerophosphate; 1 mM $Na_3VO_4$; 1 mM PMSF. Approximately 1 mg of total protein from each sample group was

immunoprecipitated using 6 μg of anti-RPA-p34 antibodies (Bethyl Laboratories, Inc., Montgomery, TX) cross-linked to 60 μL of protein G-agarose beads (Invitrogen, Carlsbad, CA). The antibodies were cross-linked to the beads by incubating them together for 1 h at room temperature with end-over-end mixing. The beads were then washed twice with 200 mM triethanolamine (Sigma-Aldrich) and then incubated in 20 mM dimethylpimelimidate (DMP; Sigma-Aldrich) in 200 mM triethanolamine for 30 min at room temperature. The DMP solution was replaced with 50 mM Tris-HCl, pH 7.5 for an additional 15 min. The Tris-HCl was removed, and the cell lysates were then added to the beads. Following 14–16 h incubation at 4 °C with end-over-end mixing, the immunoprecipitates were washed once with PBS, and the proteins were then eluted from the beads using 250 μL of 2D rehydration buffer (7 M urea; 2 M thiourea; 4% CHAPS; 40 mM DTT; 2.0% IPG buffer).

### First Dimension/Isoelectric Focusing

For recombinant RPA, approximately 1.5 μg of either rhRPA or hypRPA were mixed with 250 μL of 2D rehydration buffer. For HeLa lysates, the proteins were eluted from the immunoprecipitation reaction using the 2D rehydration buffer. The protein-containing rehydration buffer was placed in 13-cm strip holders (Amersham Biosciences, Buckinghamshire, England), and Immobiline DryStrip polyacrlyamide strips with an immobilized pH gradient of pH 3–10 (Amersham Biosciences) were immersed in the buffer; 1.5 mL of mineral oil was layered on top of each strip, the cover was added, and the holders were then placed in a Pharmacia Biotech IPGphor isoelectric focusing system (Amersham Biosciences) under the following conditions: 20 °C, 50 μA/strip. The electrophoretic program was run in four steps: Step 1–50 V, 12 h; Step 2–500 V, 1 h; Step 3–1000 V, 1 h; Step 4–8000 V, 8h.

### Second Dimension Gel Analysis

Following isoelectric focusing, the strips were removed from the strip holders, rinsed in $dH_2O$, and then incubated in equilibration buffer 1 for 15 min at room temperature (50 mM Tris-HCl, pH 8.8; 6 M urea; 30% glycerol; 2% SDS; 1% DTT). The strips were then transferred to equilibration buffer 2 (50 mM Tris-HCl, pH 8.8; 6 M urea; 30% glycerol; 2% SDS; 2.5% iodoactamide) and incubated for an additional 15 min at room temperature. The strips were placed on top of 12% polyacrlyamide SDS gels with 0.5% agarose layered on top of the strips. The 2D gels were electrophoresed at 16 °C for 15 min at 10 mA/gel and 300 V; then 25 mA/gel and 300 V for 5 h.

## RESULTS

### Purification of in Vitro Hyperphosphorylated RPA

The posttranslational modification of RPA has been the subject of intense study (25, 28). Specifically, numerous sites of phosphorylation on the N-terminus of the p34 subunit have been implicated in regulation of RPA activity and its role in DNA metabolic pathways (16, 29–31). To better characterize potential sites of phosphorylation and to aid in development of methodologies for identification of novel sites of phosphorylation, we have prepared and purified an in vitro hyperphosphorylated form of RPA. Partially purified RPA produced in *E. coli* was incubated with HeLa crude extracts in the presence of a cocktail of phosphatase

inhibitors to allow the kinases within the extracts to phosphorylate RPA. While the promiscuous nature of kinases may result in the in vitro phosphorylation of a site(s) that may not be a bona fide in vivo site of modification, this procedure should allow us to identify an array of sites that can then be confirmed using in vivo phosphorylated RPA. Following in vitro phosphorylation, the resulting hyperphosphorylated RPA was purified identically to RPA as we have previously described (27). SDS–PAGE of Q-Sepharose fractions of the hyperphosphorylated RPA reveals the difference in migration of the phosphorylated p34 subunit of the hyperphosphorylated RPA compared with the control RPA (Figure 1A). Western blot analysis of fractions from the purification demonstrates that, prior to incubation with HeLa crude extracts in the presence of phosphatase inhibitors, the p34 subunit runs as a single band on a SDS–PAGE gel (Figure 1B, lane 1). Following the incubation with the cell extract in the presence of phosphatase inhibitors, multiple bands or forms of RPA-p34 exist that represent different levels of phosphorylation. The final pool of hyperphosphorylated RPA is characterized by p34 bands that migrate more slowly in the gel and are consistent with the presence of Form 5 (17). Incubation of the hyperphosphorylated RPA with CIP results in a migration similar to that of the untreated RPA (Figure 1B).

## Investigation of Sites of Modification: Phosphospecific Antibodies

To determine the extent of RPA phosphorylation, we first set out to confirm known phosphorylation sites identified in other systems. In vitro purified phosphorylated RPA was separated by SDS–PAGE, transferred to PDVF, and probed using phosphospecific antibodies. The results presented in Figure 2 reveal that serine 33, serines 4 or 8, and threonine 21 are all phosphorylated in the preparation (Figure 2A, lanes 1, 3 and 5). Prior treatment of the RPA preparation with CIP resulted in the loss of antibody reactivity for each site (Figure 2A, lanes 2, 4 and 6) while also resulting in an increased mobility on the SDS gel (panel B). While these results demonstrate that in the pool of phosphorylated protein each of these sites is phosphorylated, these analyses cannot determine if the sites are concurrently phosphorylated, that is, all sites are phosphorylated on a single RPA protein. The design of this experiment required larger quantities of total protein to be loaded on the gel and longer exposures to allow detection with the phosphospecific antibodies. This resulted in a loss of resolution such that it was difficult to resolve Forms 3–5. Therefore, we cannot assess if phosphorylation of these specific amino acids is present exclusively in Form 5 p34 or if they are also present in Forms 3 and 4.

## Sites of Modification of Hyperphosphorylated RPA on the p34 Subunit

To confirm these sites of phosphorylation on hyperphosphorylated RPA and to ascertain the extent of phosphorylation on any given p34 subunit, we employed a procedure involving exhaustive solution digestion of the heterotrimeric RPA with trypsin followed by HPLC fractionation and MALDI-TOF MS analysis of the resulting peptides. Confirmation of specific peptide phosphorylation was achieved by separation of the RPA subunits by SDS–PAGE and in-gel digestion of the subunits with trypsin followed by HPLC and MALDI-TOF MS analysis. On-chip phosphatase treatment of the peptides was used to confirm the existence of specific phosphopeptides.

Initial analyses were performed by digesting purified hyperphosphorylated heterotrimeric RPA in solution with trypsin. The digested protein sample was fractionated by reverse phase HPLC, and each individual fraction was analyzed by MALDI-TOF MS. Each fraction was also subjected to CIP treatment prior to MS analysis. Loss of a phosphate from a peptide is expected to generate peaks differing in *m*/*z* by 80 Da. Therefore, the loss of specific peaks upon CIP treatment and generation of new peaks or enhanced peak heights corresponding to multiples of 80 Da was used identify fractions that potentially contained phosphopeptides. The results presented in Figure 3 indicated that a peptide in fraction 39 potentially contained multiple sites of phosphorylation. The MS analysis of fraction 39 identified multiple peptides that, upon treatment with CIP, reduced the spectrum to two peaks with masses of 3631.8 and 3860.1 Da. However, the tryptic peptide predicted from the N-terminus of p34 does not correspond to the observed molecular weights in fraction 39. The possibility exists that another region of RPA, potentially on other subunits of the protein, could contain multiple phosphorylation sites within a specific peptide. However, there are no predicted tryptic peptides from any of the three subunits of RPA that have theoretical masses that correspond to the CIP-resistant peptides observed in fraction 39. To investigate the identities of the unknown peptides, we purified each of the subunits of hyperphosphorylated RPA by SDS–PAGE. The bands corresponding to each subunit were excised and in-gel digested with trypsin. While every attempt was made to obtain Form 5 p34, we cannot rule out the possibility that the band excised also contained Form 4 p34. The digests were again fractionated by reverse phase HPLC and fractions were analyzed by MALDI-TOF MS. In fraction 38 of the RPA-p34 digest a phosphate ladder was again observed (Figure 3B). CIP reduced the spectrum to two prominent peaks with molecular masses of 3388.2 and 3631.2 Da (Figure 3B), and a low intensity peak with a measured molecular mass of 3260.8 Da was also observed (data not shown). Search of molecular weights of the CIP-resistant peaks revealed that they were consistent with tryptic fragments corresponding to the N-terminal peptide spanning amino acids 4–40 of RPAp34. Interestingly, there is no basic residue at the third position of RPAp34 that would produce tryptic fragments starting at the fourth amino acid. Control experiments conducted on the recombinant protein revealed that no cleavage occurred at position three. Rather, peptides corresponding to residues 1–37, 1–38, and 1–40 were observed (data not shown). We conclude that treatment with HeLa cell extracts leads to the removal of the RPA p34 N-terminal three residues. The data also demonstrate that four concurrent sites of phosphorylation occur on the N-terminus of RPAp34 (residues 4–40). We did not observe a peptide in any of the analyses that would be consistent with five concurrent phosphorylation events on a single RPA p34 N-terminal peptide.

The possibility that other portions of RPA p34 or subunits of RPA are also targets for posttranslational modification was investigated. Analysis of additional HPLC fractions of the RPA p34 digest identified a possible phosphorylated peptide in fraction 29. MALDI-TOF MS analysis of fraction 29 yielded a peptide with a measured mass of 1414.1 Da (Figure 3C). Treatment of the fraction with CIP eliminated the peak at 1414.1 and increased the intensity of a peak with a mass of 1334.6 Da (Figure 3C). This 80 Da reduction is again indicative of a singly phosphorylated peptide. Search of potential tryptic peptides yielded only a single possibility for the identity of the peptide. A peptide corresponding to residues 94–105 from RPA p34 has a theoretical mass of 1334.5 Da. This peptide contains only one

residue capable of being phosphorylated, threonine 98, and we conclude that in the hyperphosphorylated form of RPA, this residue is phosphorylated. Phosphorylation of threonine 98 was also observed in LC MS/MS analysis of hyperphosphorylated RPA p34 (Tsaprailis, Liebler, and Dixon, unpublished results).

## Determination of Sites of Phosphorylation of the p70 Subunit of RPA 70

While much attention has been devoted to phosphorylation of the p34 subunit, in yeast the p70 subunit is also phosphorylated (23, 25). Analysis of HPLC fractions generated from in-gel trypsin digestion of in vitro hyperphosphorylated RPA p70 by MALDI-TOF MS revealed the potential phosphorylation of a peptide with a molecular mass of 4458.9 Da (Figure 4A, dotted trace). Treatment of the fraction with CIP confirmed a one-phosphate modification of the peptide (Figure 4A, black trace). In another solution digestion experiment in which less trypsin was used, a similar phosphorylation event was observed. Peptides with molecular masses of 4459.9 and 5038.4 Da were observed in fraction 43 (Figure 4B, dotted trace), and CIP treatment confirmed the peaks as phosphorylations. The larger peptide includes a missed cut site at position 157 with the measured masses of the CIP-resistant peptides agreeing well with the theoretical molecular weights of tryptic peptides 112–157 and 112–163 from RPA p70. Both peptides contain a single methionine residue, and peptides corresponding to a single methionine oxidation are also observed for each peptide and serves to confirm the assignment of each peptide. There are multiple sites that could be phosphorylated within this peptide including proline-directed sites.

Additional sites of phosphorylation within the RPA p70 subunit were also detected within the C-terminal domain. A potential phosphate ladder was observed in HPLC fraction 45 of the solution digested in vitro hyperphosphorylated RPA (Figure 4C). CIP treatment reduced the ladder to two peaks with masses of 3861.0 and 3877.2 Da. The measured masses agree with the theoretical molecular weights of tryptic peptide 569–600 (3862.5 Da) and this peptide's methionine oxidation product (3878.5). This peptide contains four potential residues capable of being phosphorylated: serine 569, threonine 580, serine 585, and threonine 590 and a single methionine. The peptide is unusually trypsin resistant as it contains six missed trypsin cleavages. In a separate solution digestion experiment, a three-phosphate modification that also displayed a methionine oxidation signature was observed in HPLC fraction 44. CIP treatment of this fraction produced a peptide that was mapped to 574–604, based on accuracy of mass measurement (data not shown). This peptide lacks serine 569 but contains threonine 580, serine 585, and threonine 590. These data demonstrate that in hyperphosphorylated RPA serines 560 and 585 and threonines 580 and 590 are phosphorylated. Interestingly, this domain of RPA70 is as highly phosphorylated as the N-terminal region of the p34 subunit. We were unable to identify any fractions that would be consistent with phosphorylation of the 14 kDa subunit of RPA.

## In Vivo Phosphorylation of RPA in Response to DNA Damage

Having identified a series of phosphorylation sites in both the 70 and 34 kDa subunits present on the in vitro hyperphosphorylated RPA, we sought to confirm these sites on the in vivo phosphorylated form of RPA. Exponentially growing HeLa cells were first subjected to aphidicolin treatment to arrest cells in S-phase and at the G1/S boundary. Cells were then

released from the aphidicolin block, allowed to enter S-phase, and subsequently treated with hydroxyurea, which induces replication fork stalling and "replication stress", or UV light to induce DNA damage. The RPA modification from these treatments was compared to the in vitro hyperphosphorylated RPA by Western blot analysis and 2D gel electrophoresis. Single dimensional SDS–PAGE analysis presented in Figure 5 reveals that lysates prepared from untreated control cells contain predominantly Form 1 RPA, although there are clearly detectable levels of Forms 2–5. Both HU and UV treatment of HeLa cells result in a majority of RPA being in the hyperphosphorylated form and consistent with Form 5 RPA (17). Analysis of the in vitro phosphorylated RPA reveals that the majority of the RPA is present in Form 4 and 5 and there are minimal amounts of Form 1–3 isoforms (Figure 5A). The final three lanes present rhRPA purified from *E. coli* which migrates as a single band consistent with Form 1. Analysis of the three phosphorylated RPA species by 2D electrophoresis reveals that RPA from HU- and UV-treated cells contain many identical spots in addition to some differences (Figure 5B). Analysis of the in vitro hyperphosphorylated RPA presents a somewhat different pattern, the most noticeable difference being the lack of immunoreactivity in the basic pI and faster migrating bands indicative of the low levels of Forms 1–3 compared to the HU- and UV-treated cells. These data are consistent with the single dimension SDS–PAGE analysis of the three phosphorylated forms of RPA. A similar pattern of spots is observed focusing on species migrating more slowly in the second dimension and at acidic pI's (Figure 5C). These spots are consistent with the more highly phosphorylated forms of RPA, and the spots observed in both in vitro phosphorylated RPA and RPA in UV-treated cells are indicated by the arrows in panel C. These data suggest that the in vitro hyperphosphorylated form of RPA has similar positions of modification and degrees of modification.

Analysis of phosphorylation of the p34 subunit in HU-treated cells was assessed using phosphospecific antibodies. The results presented in Figure 6 demonstrate that each serine 33, serine 4–8, and threonine 21 is phosphorylated in this preparation. Interestingly, CIP treatment of the fraction revealed that antibody reactivity with the serine 4–8 and threonine 21 was abrogated following CIP-catalyzed removal of the phosphates. However, the antibody to phosphoserine 33 was able to detect a RPA p34 subunit that migrated faster than the hyperphosphorylated Form 5 RPA in the gel. These results suggest that, in the in vivo phosphorylated RPA p34, serine 33 is resistant to phosphatase treatment. The increase in signal intensity after phosphatase treatment (compare lanes 1 and 2) was variable and may be a function of the specificity of the antibody or potential inhibitory effect of other sites of phosphorylation within the N-terminus of in vivo hyperphosphorylated RPA. While the antibody reactivity was fairly robust, we sought to confirm the sites of modification and phosphatase resistance using MALDI-TOF MS analysis.

RPA was purified from extracts prepared from HU-treated cells and sites of phosphorylation analyzed as described for the in vitro phosphorylated RPA. Analysis of the p34 subunit revealed a series of interesting results. A series of phosphatase-sensitive peaks were identified in the HPLC fraction that corresponded to the N-terminus of p34. Three peptide peaks were observed that upon CIP treatment were lost. Interestingly, the *m*/*z* of the CIP-treated peak did not correspond to a completely phosphate-free peptide. Instead, a mass

consistent with a peptide corresponding to residues 3–37 containing two phosphates was observed (Figure 7A). The three peaks observed without CIP treatment corresponded to increases in mass of 80, 160, and 240 Da representing three, four, and five phosphorylated sites, respectively. The majority of the p34 N-terminus, however, comprises the three and four phosphorylated species with the five phosphates representing a minority of the total p34.

Having confirmed multiple sites of N-terminal phosphorylation, we assessed the phosphorylation of the p70 subunit. Analysis of HPLC fractions corresponding to the peptide consisting of amino acids 112–157 revealed phosphorylation of a single residue within this peptide. These results demonstrate that in vivo the p70 subunit of RPA is phosphorylated (Figure 7B). As mentioned earlier, this peptide contains a number of potential phosphorylation sites in close proximity to a number of proline residues suggesting that p70 phosphorylation may be catalyzed by a proline-directed protein kinase.

We were unable to detect phosphorylation of the other sites identified in the in vitro phosphorylated RPA, specifically threonine 98 in the p34 subunit and the C-terminal domain of p70, in the RPA purified from HU-treated cells. This inability could be a result of the site being phosphorylated to a low level and in the background of a large amount of unphosphorylated protein the modifications were below our detection limit. However, we were able to clearly detect the parent fragments (data not shown), and there was minimal background noise in the spectrum that would influence the detection. Alternatively, these sites could be phosphorylated in vivo in response to other stimuli, i.e., cell cycle progression or other DNA metabolic events.

## DISCUSSION

The posttranslational phosphorylation of RPA during the normal cell cycle and in response to DNA damage is well established. How these modifications alter the role of RPA in the many DNA metabolic pathways in which it participates remains largely unknown. Recently, we have demonstrated that an intermediately phosphorylated form of RPA specific to the mitotic phase of the cell cycle displayed a decrease in duplex DNA binding/destabilization activity but displayed no difference in binding to pyrimidine-rich single-stranded DNA (16). In support of this finding, a subsequent study utilized a mutant form of RPA in which eight serine residues were replaced by aspartic acid to mimic N-terminal phosphorylation of the p34 subunit of RPA, and this mutant also displayed a decrease in duplex DNA destabilization activity (29). The asp8 mutant was subsequently revealed to be defective in the ability to associate with replication foci in intact cells (30). There is, however, no indication that in any phosphorylated form of RPA all eight residues are phosphorylated on a single molecule.

In this report, we have characterized a purified hyperphosphorylated form of RPA that resembles the damage specific hyperphosphorylated form of RPA as assessed by 2D gel analysis and reaction with phosphospecific antibodies (17). In addition to known sites of phosphorylation, we have demonstrated that the N-terminus of p34 contains five phosphates on a single protein molecule phosphorylated in vitro and in vivo. We have also determined

by 2D gel analysis that upon UV or HU treatment, the p34 subunit migrates with at least 6–7 different isoelectric points, suggesting that additional modifications are possible. To that end, we have determined that threonine 98 of RPAp34 is capable of being phosphorylated in vitro. In the structural analysis of the minimum trimerization core of RPA reported by Bochkarev and co-workers (32) fragments of the native protein were crystalized and the structure generated revealed that threonine 98 is completely buried (0.01 $Å^2$ of side chain exposure). Importantly, we performed the phosphorylation reactions in vitro using native heterotrimeric RPA, and threonine 98 was efficiently phosphorylated in these reactions. It is hard to envision a kinase being able to modify this side chain unless it is accompanied by a conformational change that increases the accessibility of this residue. It is important to qualify this observation in that threonine 98 is buried by the N- and C-termini of RPA p14, which are without secondary structure and are likely very mobile (32). It is possible that the trimerization structure deduced is not an accurate representation of the native heterotrimer in solution or that threonine 98 is more solvent accessible than the crystal structure indicates simply due to the dynamic nature of the regions of RPA p14 that bury it. While we were unable to detect threonine 98 phosphorylation in the in vivo phosphorylated RPA following HU treatment, it will be interesting to determine whether this modification is present on other forms of RPA, specifically that present following UV damage or in the phosphorylated mitotic form of RPA (16). Considering the observed differences in 2D gel analysis between RPA present in HU- and UV-treated cells (Figure 6), it is likely that additional sites of modification are present in the UV-induced form of RPA.

While the N-terminus of the p34 subunit is the site of numerous phosphorylation events, we have demonstrated that the p70 subunit is also phosphorylated in vitro and in vivo (Table 1). The multiple sites of phosphorylation on the p70 subunit of RPA located within the OB fold of the C-terminus of p70, DBD C, and likely play a significant role in the duplex destabilization activity of RPA. Consistent with this, the C-terminus of RPAp70 has been shown to contribute to duplex DNA binding/destabilization (33). These sites of p70 phosphorylation likely contribute to the decrease in affinity of hyperphosphorylated RPA compared with the unphosphorylated RPA for duplex DNA observed (accompanying paper in this issue; 34). While we were unable to identify phosphorylation of the OB-fold sites in vivo, the extensive phosphorylation of this region may be independent of replication stress and specific for other DNA damaging agents or events that activate a different series of proteins kinases.

While it was not possible to identify the specific site between residues 112–157 of p70, sequence analysis indicates that only two of the sites are conserved, serine 135 and serine 148, which suggest that these may represent the possible sites of phosphorylation. Analysis of potential sites of phosphorylation using NetPhos 2.0 revealed that serines 135, 139, and 149 are potential sites of modification. In addition, tandem MS analysis indicates that either serine 148 or 149 is the site of phosphorylation of the in vitro phosphorylated RPA (Tsaprailis, Liebler, and Dixon, unpublished results). This phosphorylated region of p70 is also interesting in that it is a linker region that connects DBD A to F (32). While no direct evidence exists, modification of this region could easily influence how the domains interact to facilitate DNA binding or interaction with other proteins. No phosphorylation-dependent

impairment of RPA binding activity is observed to DNA substrates where the binding is attributed almost exclusively to the DBD A and B domains. Phosphorylation-dependent differences, however, are observed where binding is thought to require additional OB folds in DBD C and D (accompanying manuscript in this issue; 34), suggesting that phosphorylation may alter the interaction of DBD domains within the heterotrimeric structure. Interestingly, in vitro Mec1-dependent phosphorylation of serine 178 of the p70 subunit has been reported in yeast (25). This occurs in the same linker region identified in our MS analysis of both in vitro and in vivo phosphorylated human RPA p70. Additional studies in yeast revealed that the efficiency of Mec1-catalyzed phosphorylation of RPA was increased when RPA was bound to single-stranded M13 DNA (22). This increased phosphorylation was not attributed to Mec1 activation by DNA ends and was proposed to be via an alteration in RPA structure. The HU-dependent phosphorylation of RPA p70 could be the result of activation of a similar pathway, specifically ATR-dependent phosphorylation in mammalian cells as has been observed for the p34 subunit (9).

The identification of sites of phosphorylation of RPA has largely focused on the N-terminus of the p34 subunit. While this is clearly an important region of the protein, the identification of other novel sites of phosphorylation, including those on the p70 subunit, will undoubtedly contribute to modulating the RPA activity. Both effects on RPA's DNA binding activity and the ability of RPA to interact with the numerous other proteins have been shown to be modified by phosphorylation (16, 22, 29, 30). Additional studies on the specific mechanistic, biologic, and structural effects of these modifications are clearly warranted. These analyses clearly will rely on knowledge of the specific sites and extent of modification that are identified in this report.

## Acknowledgments

The phospho-specific antibody to RPA p34 threonine 21 was kindly provided by Dr. Susan P. Lees-Miller at the University of Calgary.

## References

1. Li J, Kelly T. Simian virus 40 DNA replication in vitro: specificity of initiation and evidence for bidirectional replication. Mol Cell Biol. 1985; 5:1238–1246. [PubMed: 2993858]
2. Fairman M, Stillman B. Cellular factors required for multiple stages of SV40 DNA-replication in vitro. EMBO J. 1988; 7:1211–1218. [PubMed: 2841119]
3. Braun K, Lao Y, He Z, Ingles C, Wold M. Role of protein–protein interactions in the function of replication protein A (RPA): RPA modulates the activity of DNA polymerase alpha by multiple mechanisms. Biochemistry. 1997; 36:8443–8454. [PubMed: 9214288]
4. Ramilo C, Gu LY, Guo SL, Zhang XP, Patrick SM, Turchi JJ, Li GM. Partial reconstitution of human DNA mismatch repair in vitro: Characterization of the role of human replication protein A. Mol Cell Biol. 2002; 22:2037–2046. [PubMed: 11884592]
5. Golub E, Gupta R, Haaf T, Wold M, Radding C. Interaction of human rad51 recombination protein with single-stranded DNA binding protein, RPA. Nucleic Acids Res. 1998; 26:5388–5393. [PubMed: 9826763]
6. Park MS, Ludwig DL, Stigger E, Lee SH. Physical interaction between human RAD52 and RPA is required for homologous recombination in mammalian cells. J Biol Chem. 1996; 271:18996–19000. [PubMed: 8702565]

7. Perrault R, Cheong N, Wang HC, Wang HY, Iliakis G. RPA facilitates rejoining of DNA double-strand breaks in an in vitro assay utilizing genomic DNA as substrate. Int J Radiat Biol. 2001; 77:593–607. [PubMed: 11382338]
8. Aboussekhra A, Biggerstaff M, Shivji MK, Vilpo JA, Moncollin V, Podust VN, Protic M, Hubscher U, Egly JM, Wood RD. Mammalian DNA nucleotide excision repair reconstituted with purified protein components. Cell. 1995; 80:859–868. [PubMed: 7697716]
9. Zou L, Elledge SJ. Sensing DNA damage through ATRIP recognition of RPA-ssDNA complexes. Science. 2003; 300:1542–1548. [PubMed: 12791985]
10. Dart DA, Adams KE, Akerman I, Lakin ND. Recruitment of the cell cycle checkpoint kinase ATR to chromatin during S-phase. J Biol Chem. 2004; 279:16433–16440. [PubMed: 14871897]
11. Bochkarev A, Pfuetzner RA, Edwards AM, Frappier L. Structure of the single-stranded-DNA-binding domain of replication protein A bound to DNA. Nature. 1997; 385:176–181. [PubMed: 8990123]
12. Bochkareva E, Belegu V, Korolev S, Bochkarev A. Structure of the major single-stranded DNA-binding domain of replication protein A suggests a dynamic mechanism for DNA binding. EMBO J. 2001; 20:612–618. [PubMed: 11157767]
13. Bochkarev A, Bochkareva E, Frappier L, Edwards AM. The crystal structure of the complex of replication protein A subunits RPA32 and RPA14 reveals a mechanism for single-stranded DNA binding. EMBO J. 1999; 18:4498–4504. [PubMed: 10449415]
14. Niu H, Erdjument-Bromage H, Pan ZQ, Lee SH, Tempst P, Hurwitz J. Mapping of amino acid residues in the p34 subunit of human single-stranded DNA-binding protein phosphorylated by DNA- dependent protein kinase and Cdc2 kinase in vitro. J Biol Chem. 1997; 272:12634–12641. [PubMed: 9139719]
15. Zernik-Kobak M, Vasunia K, Connelly M, Anderson CW, Dixon K. Sites of UV-induced phosphorylation of the p34 subunit of replication protein A from HeLa cells. J Biol Chem. 1997; 272:23896–23904. [PubMed: 9295339]
16. Oakley GG, Patrick SM, Yao JQ, Carty MP, Turchi JJ, Dixon K. RPA phosphorylation in mitosis alters DNA binding and protein-protein lnteractions. Biochemistry. 2003; 42:3255–3264. [PubMed: 12641457]
17. Oakley GG, Loberg LI, Yao JQ, Risinger MA, Yunker RL, Zernik-Kobak M, Khanna KK, Lavin MF, Carty MP, Dixon K. UV-induced hyperphosphorylation of replication protein a depends on DNA replication and expression of ATM protein. Mol Biol Cell. 2001; 12:1199–1213. [PubMed: 11359916]
18. Barr SM, Leung CG, Chang EE, Cimprich KA. ATR kinase activity regulates the intranuclear translocation of ATR and RPA following ionizing radiation. Curr Biol. 2003; 13:1047–1051. [PubMed: 12814551]
19. McHugh MM, Yin X, Kuo SR, Liu JS, Melendy T, Beerman TA. The cellular response to DNA damage induced by the enediynes C-1027 and neocarzinostatin includes hyperphosphorylation and increases nuclear retention of replication protein A (RPA) and trans inhibition of DNA replication. Biochemistry. 2001; 40:4792–4799. [PubMed: 11294647]
20. Cheng XB, Cheong N, Wang Y, Iliakis G. Ionizing radiation-induced phosphorylation of RPA p34 is deficient in ataxia telangiectasia and reduced in aged normal fibroblasts. Radiother Oncol. 1996; 39:43–52. [PubMed: 8735493]
21. Lees-Miller SP, Anderson CW. The DNA-activated protein kinase, DNA-PK: a potential coordinator of nuclear events. Cancer Cells. 1991; 3:341–346. [PubMed: 1751287]
22. Clifford DM, Marinco SM, Brush GS. The meiosis-specific protein kinase Ime2 directs phosphorylation of replication protein A. J Biol Chem. 2004; 279:6163–6170. [PubMed: 14634024]
23. Brush GS, Morrow DM, Hieter P, Kelly TJ. The ATM homologue MEC1 is required for phosphorylation of replication protein A in yeast. Proc Natl Acad Sci, USA. 1996; 93:15075–15080. [PubMed: 8986766]
24. Brush GS, Anderson CW, Kelly TJ. The DNA-activated protein kinase is required for the phosphorylation of replication protein A during simian virus 40 DNA replication. Proc Natl Acad Sci, USA. 1994; 91:12520–12524. [PubMed: 7809070]

25. Kim HS, Brill SJ. MEC1-dependent phosphorylation of yeast RPA1 in vitro. DNA Repair. 2003; 2:1321–1335. [PubMed: 14642562]
26. Block WD, Merkle D, Meek K, Lees-Miller SP. Selective inhibition of the DNA-dependent protein kinase (DNA-PK) by the radiosensitizing agent caffeine. Nucleic Acids Res. 2004; 32:1967–1972. [PubMed: 15060176]
27. Patrick SM, Turchi JJ. Replication protein A (RPA) binding to duplex cisplatin-damaged DNA is mediated through the generation of single-stranded DNA. J Biol Chem. 1999; 274:14972–14978. [PubMed: 10329699]
28. Wang HY, Guan J, Wang HC, Perrault AR, Wang Y, Iliakis G. Replication protein A2 phosphorylation after DNA damage by the coordinated action of ataxia telangiectasia-mutated and DNA- dependent protein kinase. Cancer Res. 2001; 61:8554–8563. [PubMed: 11731442]
29. Binz SK, Lao Y, Lowry DF, Wold MS. The phosphorylation domain of the 32-kDa subunit of replication protein a (RPA) modulates RPA-DNA interactions – Evidence for an intersubunit interaction. J Biol Chem. 2003; 278:35584–35591. [PubMed: 12819197]
30. Vassin VM, Wold MS, Borowiec JA. Replication protein A (RPA) phosphorylation prevents RPA association with replication centers. Mol Cell Biol. 2004; 24:1930–1943. [PubMed: 14966274]
31. Pan ZQ, Park CH, Amin AA, Hurwitz J, Sancar A. Phosphorylated and unphosphorylated forms of human single-stranded DNA-binding protein are equally active in simian virus 40 DNA replication and in nucleotide excision repair. Proc Natl Acad Sci, USA. 1995; 92:4636–4640. [PubMed: 7753855]
32. Bochkareva E, Korolev S, Lees-Miller SP, Bochkarev A. Structure of the RPA trimerization core and its role in the multistep DNA-binding mechanism of RPA. EMBO J. 2002; 21:1855–1863. [PubMed: 11927569]
33. Lao Y, Lee C, Wold M. Replication protein A interactions with DNA. 2 Characterization of double-stranded DNA-binding/helix-destabilization activities and the role of the zinc-finger domain in DNA interactions. Biochemistry. 1999; 38:3974–3984. [PubMed: 10194309]
34. Patrick SM, Oakley GG, Dixon K, Turchi JJ. DNA damage induced hyperphosphorylation of replication protein A 2. Characterization of DNA binding activity, protein interactions, and activity in DNA replication and repair. Biochemistry. 2005; 44:8428–8437. [PubMed: 15938632]
35. Block WD, Yu Y, Lees-Miller SP. Phosphatidyl inositol 3-kinase-like serine/threonine protein kinases (PIKKs) are required for DNA damage-induced phosphorylation of the 32 kDa subunit of replication protein A at threonine 21. Nucleic Acids Res. 2004; 32:997–1005. [PubMed: 14872059]

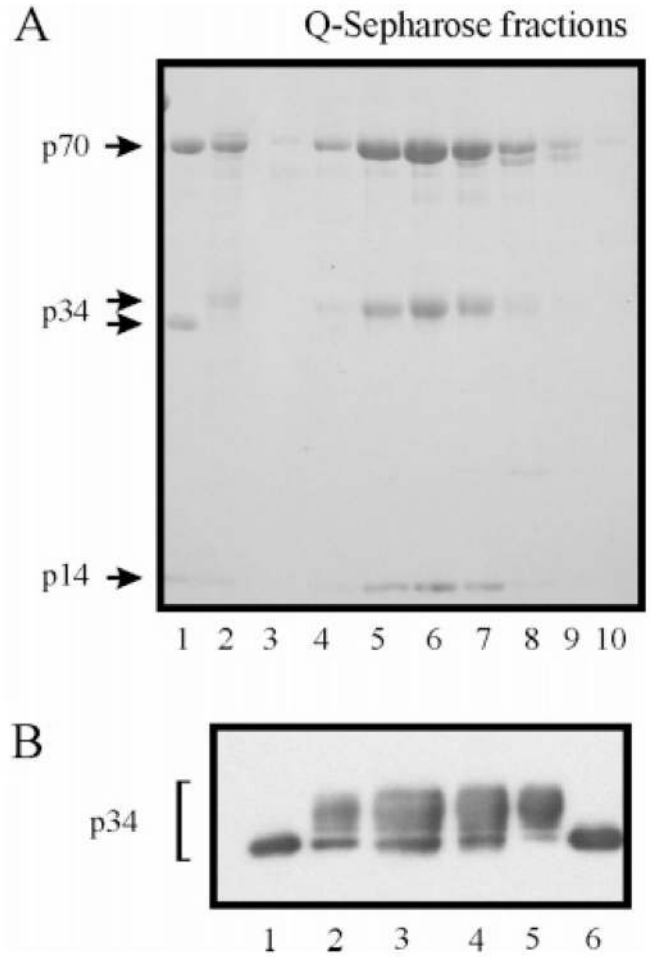


**Figure 1.**

Purification of in vitro hyperphosphorylated RPA. The purification of hyperphosphorylated RPA was performed using the same chromatographic procedures as for rhRPA. The final step in the purification was performed using a Q-Sepharose column. (A) Protein fractions were collected and visualized on a 13% SDS polyacrylamide gel by Coomassie Blue staining. Purified rhRPA (lane 1) and an aliquot of the material loaded on the Q-Sepharose column (lanes 2) were included as controls. Fractions eluted from the Q-Sepharose column are loaded with equal volume (lanes 3–10). The positions of the p70, p34, and p14 RPA subunits are indicated by arrows. (B) Western blot analysis of RPA fractions using the RPA-p34 monoclonal antibody. Lane 1 is the partially purified rhRPA prior to incubation with HeLa crude extracts in the presence of phosphatase inhibitors. Analysis of the sample after incubation of the crude extracts in the presence of phosphatase inhibitors (lane 2), Affi-gel blue pool (lane 3), hydroxylapatite pool (lane 4), Q-Sepharose pool (lane 5), and CIP-treated Q-Sepharose pool (lane 6) are presented.

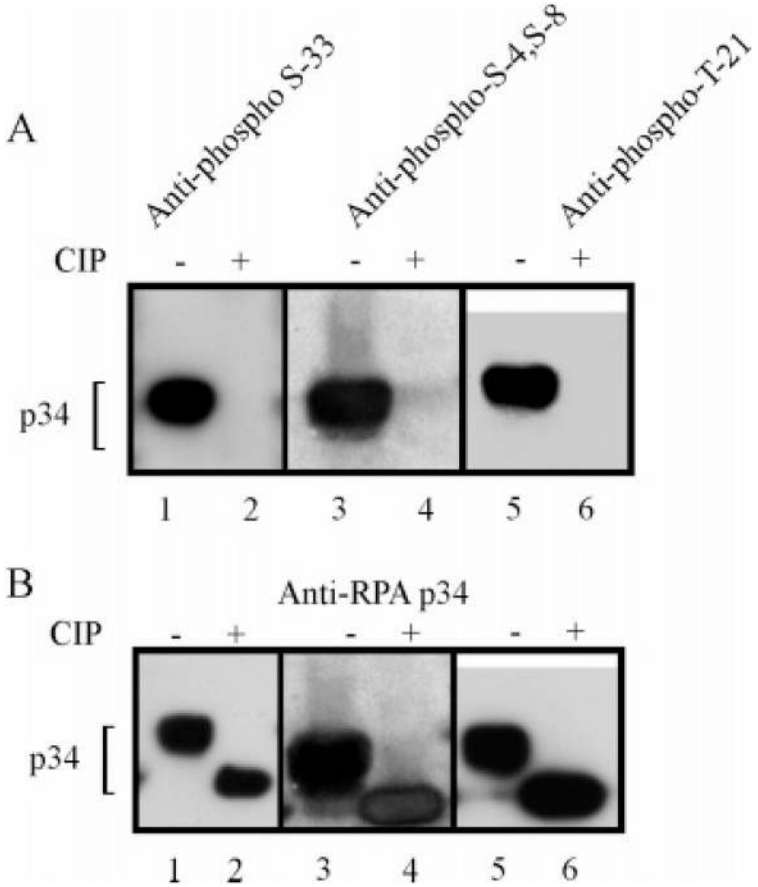


**Figure 2.**

Phosphospecific antibodies reveal multiple sites of phosphorylation on RPA p34. In vitro hyperphosphorylated RPA was purified and analyzed directly (odd lanes) or was first treated with CIP (even lanes) by SDS–PAGE and Western blot analysis. (A) Blots were probed with the indicated p34 phosphospecific antibodies. (B) Blots were stripped and reprobed with a monoclonal antibody directed against the p34 subunit which detects all forms of RPA.

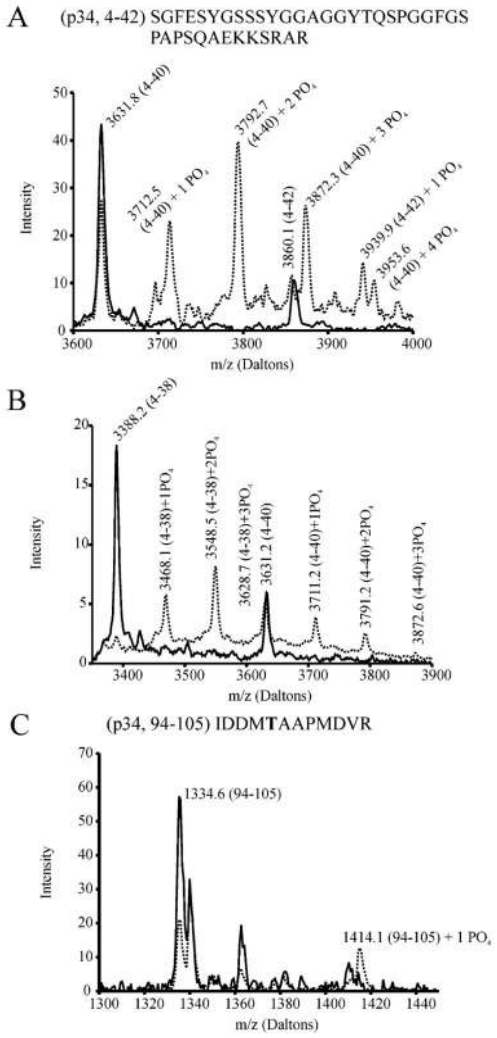


**Figure 3.**

Mass spectral analysis reveals that the N-terminus of RPA p34 contains at least four independent phosphorylations. (A) Analysis of fraction 39 from the HPLC separation of the solution digest of in vitro hyperphosphorylated RPA indicated that this fraction contained N-terminal peptide corresponding to amino acids 4–42 of the p34 subunit. This fraction was analyzed directly by MALDI-TOF MS (dotted line) or following on-chip treatment of the sample with CIP (solid line). (B) Analysis of the HPLC fractions from the separation of the in-gel digested hyperphosphorylated RPA p34 subunit indicated that fraction 38 contained the peptide corresponding to the p34 N-terminus. This fraction was analyzed directly by MALDI-TOF MS (dotted line) or following on-chip treatment of the sample with CIP (solid line). (C) In vitro phosphorylation of threonine 98 of RPA p34. Analysis of HPLC fraction 29 indicated the presence of a peptide corresponding to amino acids 94–105 of the p34 subunit. MALDI-TOF MS was performed directly (dotted line) or following CIP treatment (solid line). The *m*/*z* values, peptide, and modifications corresponding to each peak are indicated in each panel.

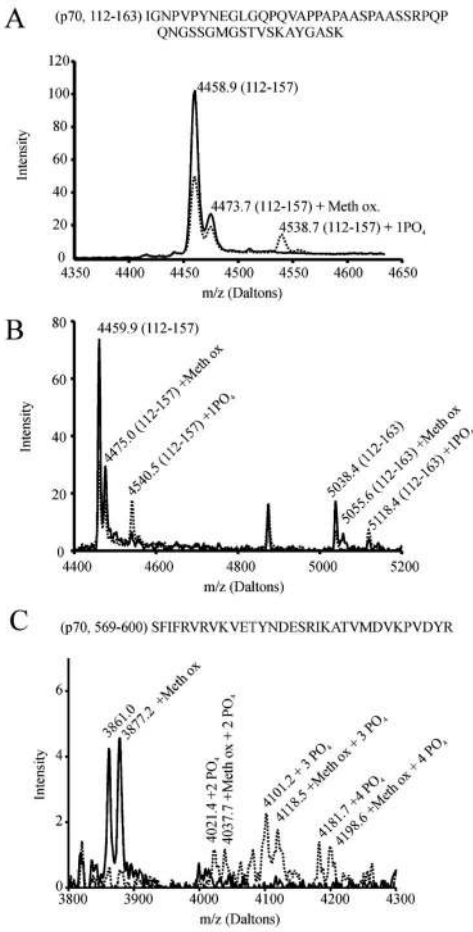


**Figure 4.**

Mass spectral analysis reveals the interdomain region and the C-terminal domain of RPA p70 is phosphorylated in vitro. (A) MALDI-TOF mass spectra of HPLC fraction 43 before (dotted) and after CIP treatment (solid) reveals the presence of a phosphopeptide. The mass of the CIP-resistant peak is consistent with tryptic peptide 112–157 from RPA p70. (B) In a separate experiment an additional phosphorylated peak is observed in fraction 43. Treatment of the fraction with CIP confirms the phosphorylation of peptide 112–163 from RPA p70. (C) Mass spectral analysis reveals the C-terminal domain from RPA p70 contains up to four phosphorylations. A phosphate ladder is observed in the MALDI-TOF mass spectrum of HPLC fraction 45 (dotted line). CIP treatment reduces the spectrum to two peaks (solid line) that are identified as peptide 569–600 and this peptide's methionine oxidation product. The *m*/*z* values, peptide, and modifications corresponding to each peak are indicated in each panel.

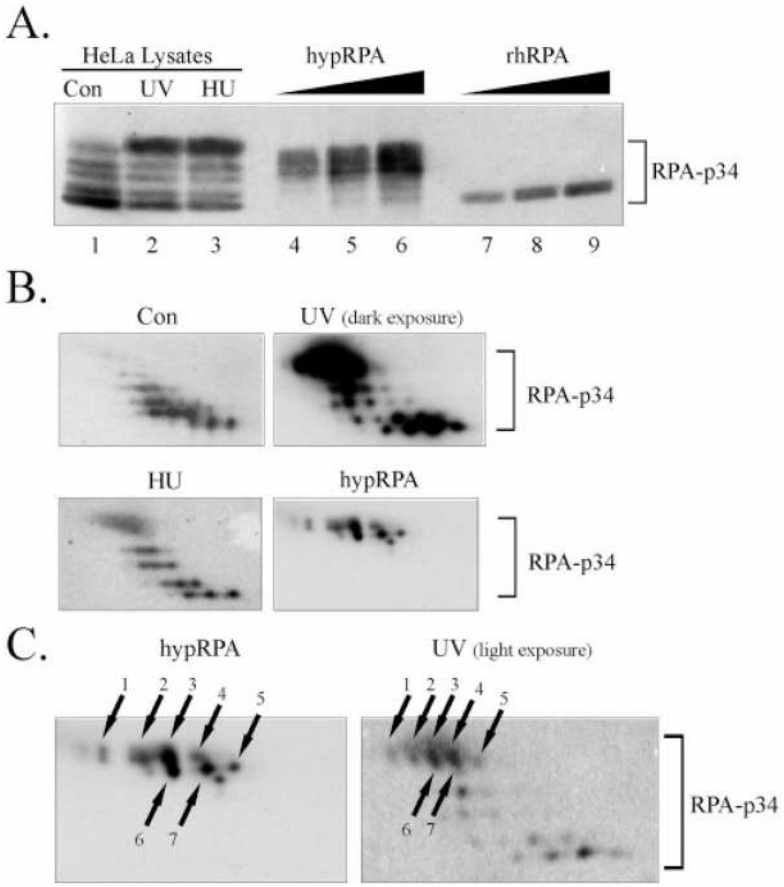


**Figure 5.**

One- and two-dimensional SDS–PAGE of HeLa and rhRPA demonstrates the presence of multiple RPA-p34 phosphorylations. HeLa cells were treated as described in Materials and Methods and lysates were prepared and probed for RPA-p34. (A) One-dimensional SDS–PAGE and Western blot analysis of extracts prepared from control (lane 1), UV (lane 2), and HU (lane 3) treated cells. Increasing concentrations of purified in vitro hyperphosphorylated RPA (lanes 4–6) or rhRPA (lanes 7–9) were also included on the gel for reference. (B) HeLa lysates (same lysates as depicted in A) and purified hyperphosphorylated RPA were separted by two-dimensional gel electrophoresis as described in Materials and Methods and probed for RPA p34. (C) Enlarged picture of 2D SDS–PAGE of hypRPA and HeLa UV-treated lysates for comparison. Arrows indicate spots that appear to migrate in a similar pattern.

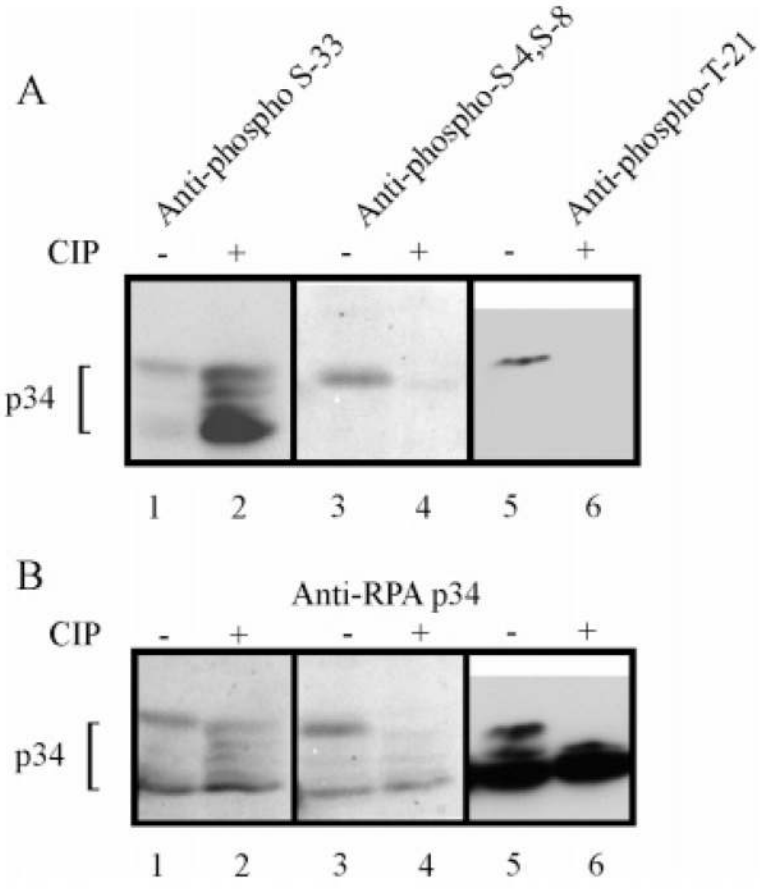


**Figure 6.**

Phosphospecific antibodies reveal multiple sites of phosphorylation on RPA p34 in response to DNA damage. Extracts prepared from HU-treated cells were analyzed directly (odd lanes) or following CIP treatment (even lanes) by SDS–PAGE and Western blot analysis. (A) Blots were probed with the indicated p34 phosphospecific antibodies. (B) Blots were stripped and reprobed with a monoclonal antibody directed against the p34 subunit of RPA which detects all forms of RPA.

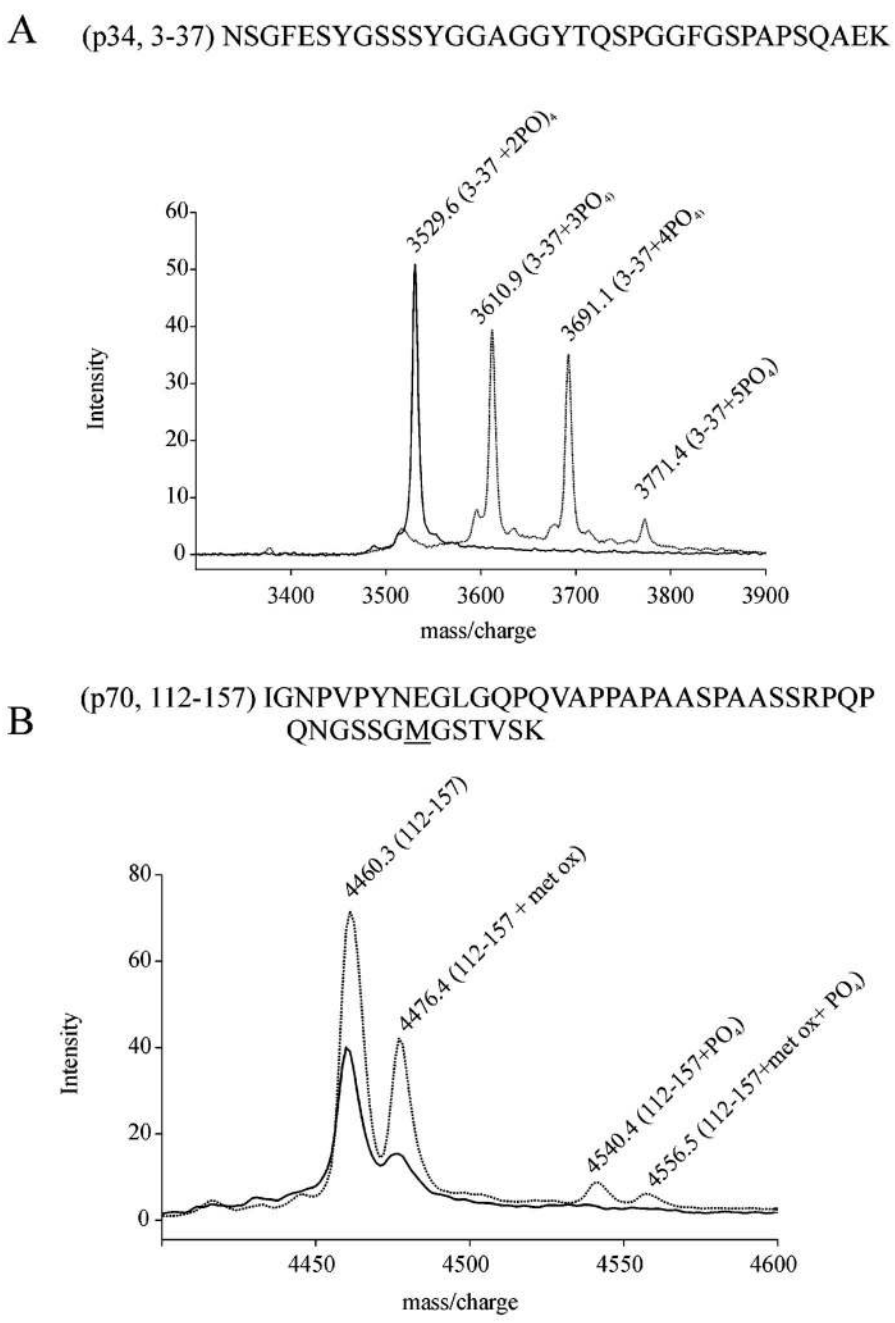


**Figure 7.**

Identification of in vivo sites of RPA phosphorylation in response to HU. RPA was purified from HeLa cells treated with HU as indicated in Materials and Methods. The protein was separated by SDS–PAGE, and the p70 and p34 subunits were excised, and subjected to in-gel trypsin digestion, HPLC fractionation, and MALDI-TOF MS analysis. (A) MALDI-TOF MS analysis of the HPLC fraction corresponding to the N-terminus peptide of RPAp34. The corresponding HPLC fraction was analyzed directly (dotted line) or following on-chip treatment of the sample with CIP (solid line). (B) Analysis of the HPLC fraction containing to the peptide corresponding to amino acids 112–157 from the p70 subunit. This fraction

was analyzed directly by MALDI-TOF MS (dotted line) or following on-chip treatment of the sample with CIP (solid line). The *m*/*z* values, peptide, and modifications corresponding to each peak are indicated in each panel.

**Table 1**

Sites of RPA Phosphorylation

| | | method[a] | | | |
|---|---|---|---|---|---|
| **subunit** | **sites** | **phospho-specific Ab** | **mass spectrometry** | **peptide mapping** | **ref** |
| p34 | | | | | |
| | S4,8 | X | | | this work, 15 |
| | S11,12,13 | | | X | 15 |
| | T21 | X | | X | this work, 14, 15, 35 |
| | S29 | | | X | 14, 15 |
| | S33 | | | X | this work, 14, 15 |
| | T98 | | *b* | | this work |
| p70 | | | | | |
| | 112–163 | | X | | this work |
| | 569–600 | | *b* | | this work |

[a] X = in vivo/in vitro.

[b] In vitro.